On ice cores chronologies

Frédéric Parrenin, Amaelle Landais

On ice cores chronologies

Parrenin Frédéric[a] and Landais Amaëlle[b], [a]Univ. Grenoble Alpes, CNRS, INRAE, IRD, Grenoble INP, IGE, Grenoble, France; [b]CNRS/CEA/UVSQ/UPS/IPSL/LSCE, Saint-Aubin, France

This is an update of J. Schwander, ICE CORE METHODS | Chronologies, Editor(s): Scott A. Elias, Cary J. Mock, Encyclopedia of Quaternary Science (Second Edition), Elsevier, 2013, Pages 303–310, ISBN 9780444536426, https://doi.org/10.1016/B978-0-444-53643-3.00309-5.

Abstract

Polar ice in Antarctica and Greenland is a primary archive to reconstruct Quaternary climate. An accurate chronology is necessary to exploit this archive. Dating methods can be derived from the counting of annual layers, from radioactive methods, from the comparison to other archives or from the modelling of the glacial sedimentation process. These methods being complementary, probabilistic models have been developed to combine them in an optimal way.

Keywords

Atmospheric composition; Chronology; Ice cores; Paleoclimatology; Quaternary

Key points

- Describe ice core dating methods
- Describe ice-air age/depth difference
- Describe probabilistic models to combine chronological information

Introduction

Ice cores drilled in Antarctica and Greenland (Fig. 1) provide a rich information on past climates which is known beyond the glaciology community. In the ideal case, the snow deposited on a glacier or ice sheet is buried by the following snowfall, building an undisturbed chronological precipitation record. After accessing this record by core drilling into this natural ice archive, one of the

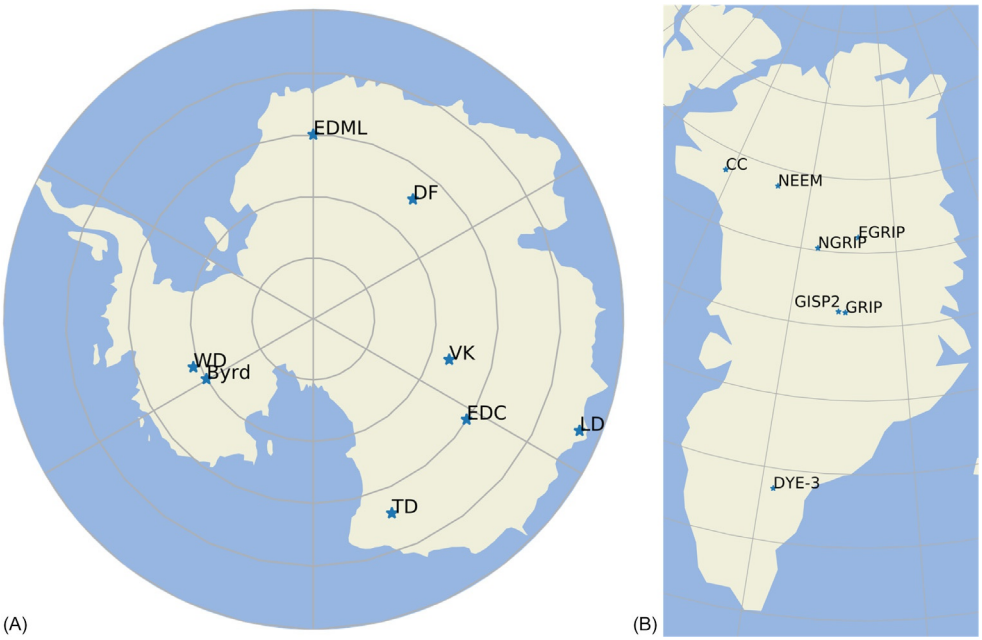

Fig. 1 Maps of the main drilling sites. (A) Antarctica: EPICA Dome C (EDC), Vostok (VK), Dome Fuji (DF), Wais Divide (WD), EPICA Dronning Maud Land (EDML), Talos Dome (TD), Law Dome. (LD), Byrd. (B) Greenland: GRIP, GISP2, DYE-3, Camp Century (CC), NorthGRIP (NGRIP), NEEM, EastGRIP (EGRIP).

first and most important tasks is to establish the ice-core chronology as precisely as possible. How well this can be done strongly depends on the climatic and ice-flow conditions at the drilling site. In this article, only cold glaciers and ice sheets, with ice body temperatures constantly below freezing, are discussed. In these ice bodies, no mass is lost by internal melting. As ice is plastically deformed under its own weight, it is generally subjected to increasing thinning with depth and age (Fig. 2A). The upper 50–150 m of an ice sheet consists of consolidated snow, commonly referred to as 'firn' (Fig. 2B). Air is continuously trapped in the lower 10% of the firn (at the firn–ice transition, the so-called lock-in-depth), where interstitial pores around the firn grains are progressively closed off until the air is permanently isolated from the overlying atmosphere. Because the firn is permeable, the air above the firn–ice transition region can exchange with the atmosphere via diffusion and convection. As a consequence, the age of the air in a sample of an ice core is younger than the age of the ice.

The main dating methods for ice cores are layer counting, radioactive dating, synchronization and ice-flow modelling. At the end, we describe how probabilistic models can help combine these different dating methods.

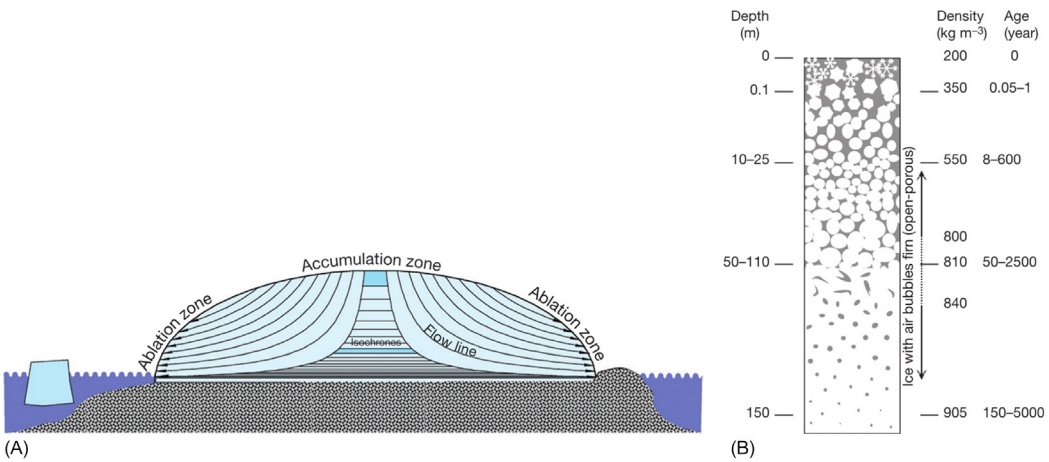

Fig. 2 (A) Schematic cross-section through an ice sheet. Layers are stretched and thinned when sinking. The two darker layers comprise roughly the same number of annual layers. (B) Firn layer of polar ice sheets: typical modern range of density and age for the top 150 m. Air bubbles are normally closed off in the density range 800–840 kg/m^3.

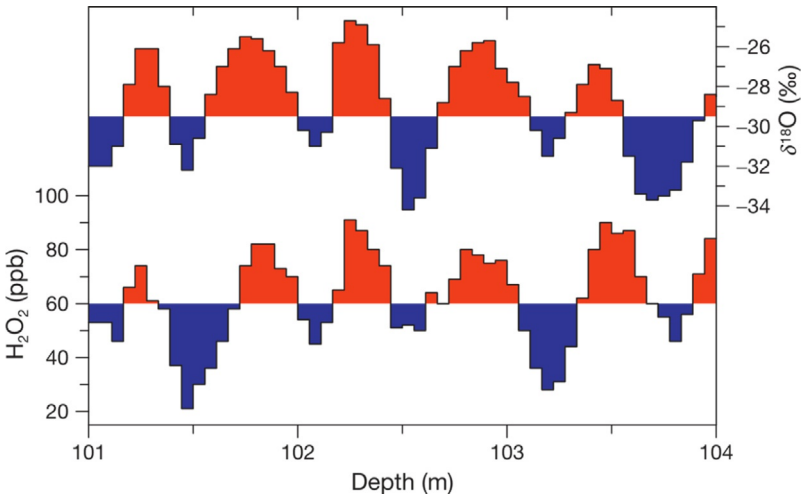

Fig. 3 Annual variations of stable isotopes (temperature proxy) and chemical trace substances (here, e.g., hydrogen peroxide, sensitive to sunlight). Summers: red, winters: blue.

Layer counting

Owing to the seasonal variation of temperature, sunlight, or atmospheric circulation, concentrations of many trace substances or isotopes show cyclic variations in ice cores (Fig. 3). If these variations occur in a regular mode and are sufficiently resolved by measurements, annual layers can be counted back many thousands of years. Depending on the conditions in the ice (temperature, thinning of layers, etc.), variations are smoothed by diffusion or altered by chemical reactions. Diffusion is especially strong in the porous firn, where the transport is enhanced through the gas phase. Diffusion processes, which can effect water isotope signals, can be corrected mathematically to a certain degree by a deconvolution algorithm, which extends the depth range for layer counting.

The classical method for tracing seasonal variations in ice cores comes from the ratio of the stable water isotopes $^{18}O/^{16}O$ and $^{2}H/^{1}H$. Since this ratio is strongly affected by the condensation temperature, it reflects the seasonal variation of temperature. Seasonal variations are preserved beyond the firn–ice transition if the annual accumulation rate is at least 200 kg/m^2. In the consolidated ice, the self-diffusion of the water molecules is much smaller than diffusive transport in the firn, and seasonal variations in the water isotopes are preserved for many thousands of years. Smoothing by self-diffusion is favored by thin annual layers (low accumulation rate, thinning by horizontal strain) and by high temperatures, for example, in the layers closer to bedrock, which are warmed by geothermal flux.

Trace substances are generally less affected by diffusion, especially when they are present in particulate form. Yet, there is always a lower limit of the annual accumulation rate, below which the annual variations are lost. One reason for this is that wind mixes the snow on the surface by scouring and relocation. Thus, annual layers are no longer preserved or are sometimes even missing. Another reason is that the annual variations are already smoothed to such a degree that when they are compacted to solid ice at the firn–ice transition, the deconvolution algorithm cannot reproduce an unequivocal record.

The best accuracy for layer counting is obtained by combining different tracers and different ice cores. An automatic algorithm for layer counting based on machine learning has also been proposed. The largest layer counting projects so far have been GICC05 for Greenland ice cores (Fig. 1) and for the last 60 kyr (kyr = 1000 years; Svensson et al., 2008) and WD2014 for the WAIS Divide ice core and for the last 31 kyr (Sigl et al., 2016).

Radioactive dating

Small amounts of radioactive trace substances are incorporated in the ice, either as deposits in the snow or trapped in air bubbles during the transition from firn to ice. As ice is a very tight container for nearly all elements (exceptions are gases with small atomic radii, e.g., helium), inclusions in cold ice are extremely well preserved. Therefore, the age can be calculated from the radioactive decay law if the initial amount of radioactive material is known. Tracers used for radioactive dating of ice are given in Table 1.

^{210}Pb

^{210}Pb is a decay product of ^{222}Rn. Its half-life of 22 years makes it suitable to date relatively young ice. As the initial content of ^{210}Pb in snow is not very constant, the method is used only when no other dating options are available.

Table 1 Radioactive isotopes used for dating ice cores.

Isotope	*Half-life (years)*
^{3}H (tritium)	12.26
^{210}Pb	22.3
^{32}Si	172
^{39}Ar	269
^{14}C	5730
^{85}Kr	10,739
^{81}Kr	229,000
^{36}Cl	301,000
^{10}Be	1,510,000
^{238}U	4,468,000,000

^{32}Si

A half-life of 172 years makes this isotope very suitable for dating historic age. But compared to other methods, it has never gained much importance because of its low and variable initial concentrations.

^{85}Kr, ^{39}Ar, ^{81}Kr, ^{40}Ar

Gases are occluded in bubbles only at a certain depth, and the age of the air is less than the age of the ice. While ^{85}Kr has been used to date the air within the permeable firn layer, ^{39}Ar would be appropriate to date the air below the firn–ice transition. However, its abundance is too small to obtain accurate ages of the air in the ice using conventional counting techniques. This problem has been overcome by new techniques such as Atom Trap Trace Analysis, which has extended the dating range for the occluded air using ^{81}Kr. The first measures needed several tens of kg of ice. They have therefore been performed on the horizontal ice core of Taylor Dome where ice older than 100 kyr is outcropped at surface. Over the last few years, technical advances have drastically reduced sample sizes. Today, 6 kg of ice can be measured to a relative age uncertainty of 10%.

The radioactive decay of ^{40}K from the terrestrial mantle leads to an increase of the concentration of ^{40}Ar in the atmosphere. By measuring the isotopic ratio ^{40}Ar/^{36}Ar (expressed using the δ^{40}Ar notation), it is therefore possible to obtain an estimate of the age of air trapped in bubbles. From the measure of δ^{40}Ar in air bubbles from the EDC ice core dated by other techniques, it has been possible to estimate an increase ratio of ~0.066‰ per million years (Bender et al., 2008), which is small relative to analytical uncertainties (0.020‰), while δ^{40}Ar is also affected by thermal and gravitational fractionation. The error associated with such method is thus important, of the order of 100 kyr at minimum typically for ice ~1 million years old. This method can also become problematic for ice situated near the bedrock, where δ^{40}Ar can be artificially increased by direct emissions from the bedrock.

^{14}C

Ice contains carbon in the form of CO_2 in the bubbles and dissolved or particulate matter (dust, pollen). Because of the small amount of ^{14}C, only measurements with accelerator mass spectrometry (AMS) are feasible with the amount of ice available from core drilling. A few measurements have been done on 10-kg samples of 6–11 kyr old ice from the Dye3 core, with an accuracy of between 5 and 10%, which is significantly less than the accuracy of other methods.

Modern radiocarbon AMS dating can be done on very small samples, for example, a few hundred pollen grains and ultimately probably even on single larger pollen grains. The method has been successfully applied on organic carbon filtrates of as little as 5 mg from an Alpine ice core.

For using ^{14}C for dating of ice, one must consider in situ production of ^{14}C by cosmogenic neutrons and muons, which interact with the oxygen of the water molecules yielding extra ^{14}CO and $^{14}CO_2$. The amount of in situ produced ^{14}C depends on cosmic ray intensity, exposure time, as well as losses by diffusion and decay. The penetration depth of neutrons and muons in firn is a few meters and a few tens of meters, respectively. At low accumulation sites with firn depths of around 100 m, most in situ produced ^{14}C has time to escape to the atmosphere before bubbles are closed off. Post-coring in situ production of ^{14}C may also be important, especially when ice cores are stored at high altitudes and latitudes, where the cosmic ray intensity is considerable.

^{10}Be and ^{36}Cl

^{10}Be and ^{36}Cl are produced by cosmic rays, which are modulated by solar activity and Earth's magnetic field. Aside from the latest drilled ice cores from Antarctica, most ice cores that have been recovered so far are significantly younger than the half-life of these isotopes. Fluctuations in the initial contents limit the dating accuracy. Since both isotopes are produced and transported by similar mechanisms, one could expect that the initial ^{10}Be/^{36}Cl ratio should be rather constant, and that this ratio, with an apparent half-life of 376 kyr, could be adequate for dating ice. However, even this ratio fluctuates by a factor of 2–5, likely due to their differing

chemical properties. Therefore, the main purpose of ^{10}Be and ^{36}Cl measurement on ice cores has been to study variations in solar activity and the Earth's magnetic field. However, in the case of disturbed layering of very old remnant ice near the bedrock, dating with these isotopes could provide rough estimates of the period during which ice was formed.

Uranium series

The measurement of ^{238}U and its daughter products has been used to determine the age of blue ice from Allen Hills, though with relatively large uncertainties. Daughter products in the ice originate predominantly from the recoiling out of dust particles into the ice due to alpha decay. The amount of the daughters that have accumulated in the ice is dependent on the length of time the particles have been incorporated in the ice. The method has been significantly improved and validated on well-dated ice samples from the Dome C ice core, and can also provide a first age estimate for basal ice. The age range of the U-series method is limited to about 1 My, at which the daughter products of ^{238}U approach equilibrium concentrations. The relative uncertainty is about 10% for intermediate ages (200–500 kyr).

Age horizons and synchronization

Since the uncertainties associated with absolute dating of ice are considerable (mainly due to the small amount of datable material), ice-core chronologies often rely on indirect dating, that is, by comparison with other better dated paleoarchives, including other ice cores. In the ideal case, the well-dated sediment record is annually laminated. Unfortunately, these varved sediments are often affected by hiatuses or do not extend to the present, but they can provide valuable information on the duration of climate events. Other archives are well suited to the application of absolute dating methods, such as U/Th-dated speleothems or corals.

The prerequisite for a correlation with ice-core records is that events occurring in the ice record are unequivocally assignable to a synchronous event in the dated record. Such events include volcanic eruptions, Milankovitch (orbital) variations, abrupt climate variations (Dansgaard–Oeschger, D-O events), variations in the Earth's magnetic field, variations in solar activity, or the impact of extraterrestrial objects.

Volcanic eruptions

Acid precipitation (mainly sulfuric acid) from volcanic eruptions can easily be identified by electric conductivity measurements and ionic analyses. Large volcanic eruptions from the equatorial zone produce a global signal (e.g., Tambora, Indonesia, 1815 CE; Fig. 4). Volcanoes at higher latitudes usually produce only hemispheric signals (e.g., Laki, Iceland, 1873 CE). Volcanic eruptions in the historic era have been used extensively to date younger ice with a 1-year accuracy and to determine mean modern accumulation rates (Sigl et al., 2015). Older volcanic eruptions are very useful for correlating different ice cores. The correlation between Northern and Southern ice cores is difficult, but has been recently performed for the last glacial period between the annually counted NorthGRIP and WAIS Divide ice cores (Svensson et al., 2020). Potentially, ice cores can be synchronized by tephrachronology if volcanic layers can be attributed unequivocally to a specific eruption, for example, by its chemical signature.

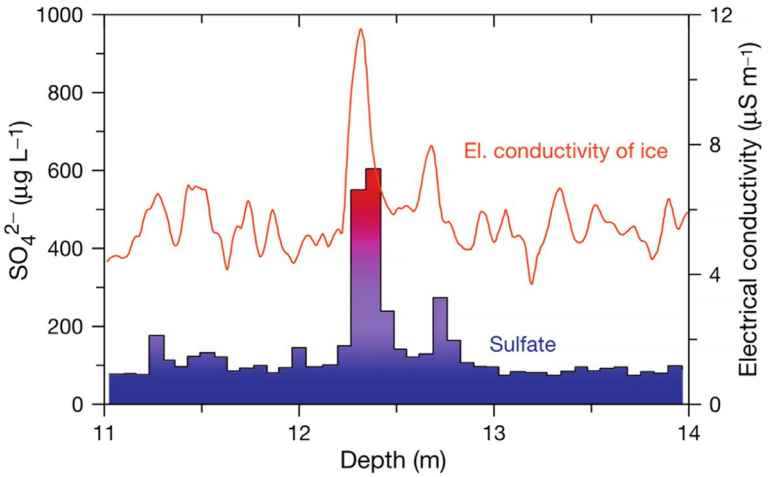

Fig. 4 The Tambora 1815 CE eruption recorded in the ice core from Dome C, Antarctica.

Tuning to astronomical cycles

In the second half of the 19th century, James Croll proposed that the Pleistocene Ice Ages are caused by periodic changes in the Earth's orbit around the Sun. These quasicyclic changes are a result of the gravitational interaction of the Earth with the Sun, the Moon, and the other planets of the solar system. Milutin Milankovitch improved the astronomical theory, leading eventually to the generally accepted theory of causality between Earth's orbital parameters and climate variations. Orbital computations have been further developed, for example, by André Berger and Jacques Laskar. Orbital variations can be determined to a precision of about 1 kyr in 1 My.

Tuning is accomplished by changing the chronology of a record such that its correlation with the target astronomical curve is increased (e.g., by maximizing the spectral power at the orbital bands). The target curve (e.g., total ice volume for tuning marine benthic $\delta^{18}O$ records) is calculated from the astronomical parameters (e.g., insolation at a given latitude) using a suitable model. A shortcoming of the method is the problem of over-tuning. For example, it has been shown that the spectral power at the Milankovitch band can be readily generated by tuning an arbitrary record of white noise. Orbital tuning work has therefore been as conservative as possible. The uncertainty in the phasing between paleorecords and the astronomical cycles varies depending on the record used.

Ice-core records can be correlated to the Milankovitch cycles either directly or indirectly via synchronization, for example, with marine sediment records that are orbitally tuned. Direct tuning includes temperature-sensitive stable isotope ratios, the $\delta^{18}O$ of oxygen in the trapped air, the O_2/N_2 ratio and the Total Air Content (TAC).

Stable isotope ratios (δD, $\delta^{18}O$) in precipitation predominantly reflect local temperature and are therefore climate sensitive. The oxygen in air bubbles ($\delta^{18}O_{atm}$) locked within an ice core depends on the ocean water $\delta^{18}O$ (hence total ice volume) as well as the hydrologic cycle of the low latitudes (where productivity is maximum) and biosphere productivity. The transfer from the ocean $\delta^{18}O$ to the air happens through the biosphere, with an offset of 23.5% (called 'Dole effect'). Fig. 5 shows the correlation between $\delta^{18}O_{atm}$ and Northern summer insolation (Extier et al., 2018), which is clear, but the problem is that the phasing between these two parameters is large (~5 kyr) and probably strongly varying in time (Extier et al., 2018). Because $\delta^{18}O_{atm}$ shares a lot of similarities with $\delta^{18}O_{calcite}$ of speleothems in the low latitudes, both records being affected by ocean water $\delta^{18}O$ and low latitude hydrologic cycle, it has therefore been proposed to tune $\delta^{18}O_{atm}$ to the U/Th-dated $\delta^{18}O_{calcite}$ record measured in East Asian speleothems (Extier et al., 2018). Because $\delta^{18}O_{atm}$ is a global parameter, it can also be used to synchronize the gas records of ice cores from both hemispheres. However, an even better candidate for this purpose is methane, because of its more distinct variations (see Section "Abrupt climate variations").

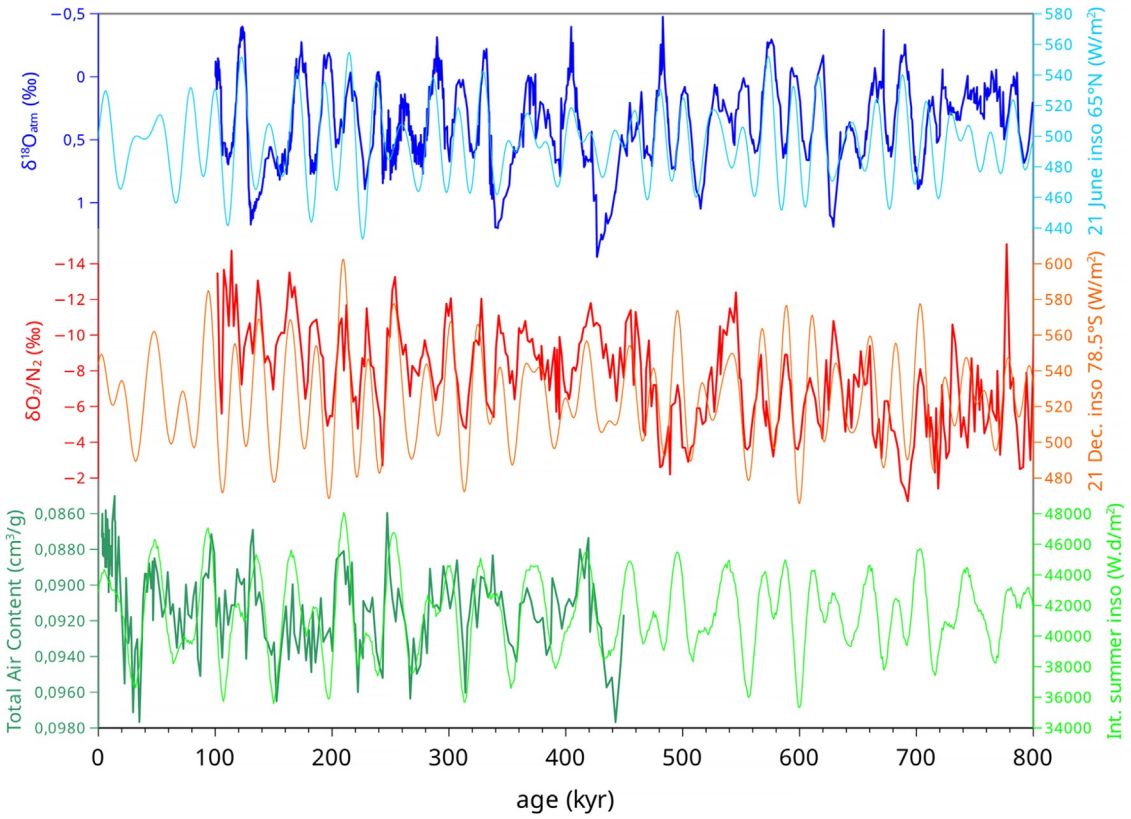

Fig. 5 3 Orbital tracers ($\delta^{18}O^{atm}$, $\delta O_2/N_2$ and TAC) on the EDC ice core, together with their insolation targets.

The O_2/N_2 ratio of the air extracted from ice cores is slightly less than the atmospheric ratio because O_2 is preferentially excluded at the firn–ice transition during the gas-trapping process. Additionally, there is usually some preferential loss of O_2 from the outer part of the ice core during storage. Bender (2002) has observed a high correlation between the O_2/N_2 ratio measured in the Vostok ice core and the local summer insolation, a relationship which has been confirmed for the Dome F and EDC ice cores (Fig. 5). Bender assumes that the summer climate influences the physical properties of the firn grains, which eventually affects exclusion of O_2 at the firn–ice transition. Although the mechanism is not well understood yet, it is most promising because of the direct link with local insolation. It should be noted that, despite the O_2/N_2 ratio being measured in the air bubbles, it actually depends on the surface conditions and is therefore a tool for the dating of the ice matrix.

It has also been shown that the TAC of ice is correlated with an integrated summer insolation (Raynaud et al., 2007), probably through a similar mechanism linking the summer climate with the properties of the firn grains at surface (Fig. 5). Therefore, despite TAC being measured in the air bubbles, it is also a tool for dating the ice matrix. The difference with O_2/N_2 is that TAC contains comparatively more obliquity frequencies compared to O_2/N_2, therefore the insolation target is integrated over a longer summer period.

Abrupt climate variations

Abrupt warmings during glacial times (the so-called Dansgaard-Oeschger events, D-O events) are observed in the Greenlandic ice cores. They are associated with rapid changes in the thermohaline circulation, with reduced deep-water formation in the North Atlantic. Temperature increases of 10 °C in Greenland occurred within the span of decades following the onset of events. D-O events are also seen in regions throughout the Northern hemisphere, albeit with a possibly smaller amplitude. Such rapid events are therefore most suitable for synchronization with other paleorecords of similar sensitivity to these abrupt changes. D-O events are accompanied by abrupt variations of the atmospheric methane concentration. Since the mixing time of Earth's atmosphere is of the order of a few years, these variations are observed in both hemispheres without considerable delay and are therefore ideal to synchronize the gas records from ice cores of the Northern and Southern Hemispheres (EPICA Community Members et al., 2006). In Greenland, the abrupt temperature changes also create a thermal fractionation of air isotopes such as ^{15}N and ^{40}Ar in the firn, which is visible in the ice core record of air bubbles (Severinghaus et al., 1998).

In the temperature records of Antarctic ice cores, D-O events translates into more gradual and anti-phased events called Antarctic Isotopic Maxima (AIM), and the timing of D-O events can still be determined by the extrema of this isotopic curve, albeit sometimes with a $\sim$ 200 yr lag (Svensson et al., 2020).

Within the same ice core, the D-O events therefore can provide a synchronization of the ice matrix (through the isotope) and of the air bubbles (through the methane or ^{15}N) which allows to determine the ice-air depth shift of synchronous events (Severinghaus et al., 1998).

The recent advances in U/Th chronologies of speleothems has allowed to determine the timing of D-O events with a great accuracy of sometimes less than 100 yr (Corrick et al., 2020; Wang et al., 2001). These dated horizons can therefore be used to date the ice phase in Greenland ice cores (through the water isotope) or the air phase in Greenland and Antarctic ice cores (through the methane concentration), as illustrated in Fig. 6.

Variations of the Earth's magnetic field

The magnetic field of the Earth has undergone substantial variations in the past, including changes in overall strength, movement of the magnetic poles, and magnetic reversals. The Laschamp event, a prominent period with substantially reduced magnetic field intensity, occurred around 41 kyr BP. A weak magnetic field causes a lower shielding of the cosmic rays, thereby leading to an increase in cosmogenic production of radionuclides. Peaks in ^{10}Be and ^{36}Cl in polar ice cores have been found to coincide with the Laschamp event (Raisbeck et al., 2007).

Variations of the solar activity

The activity of the sun shows several quasi-cyclic variations. The most prominent one is the 11-year sunspot cycle (Schwabe cycle; half period of magnetic reversal) and the associated 22-year Hale cycle (full period of magnetic reversal). Other suggested cycles are Gleissberg (88 years), Suess (200 years), and Hallstatt (2.3 kyr). There are also periods with exceptionally low solar activity (sunspot minima): these include the Dalton minimum (1790–1820 CE), the Maunder minimum (1645–1715 CE), the Spörer minimum (1450–1550 CE), and the Wolf minimum (1280–1350 CE). Changes in solar wind associated with changes in solar activity affect the magnetic field of the Earth and thus the production of cosmogenic radionuclides. The sunspot minima and the Schwabe cycle are clearly reflected in the ^{10}Be and ^{36}Cl content of ice-core records. Whether the 11-year cycle could eventually serve as a dating tool depends on the stability of its period, a question that is presently still open. An attempt to use the Schwabe cycle for dating has been made for the Tayler Dome ice core. The ^{10}Be and ^{36}Cl records can be synchronized to the atmospheric ^{14}C record, another cosmogenic radionuclide which can be reconstructed using old trees, placed on an absolute chronology of matching tree rings sequences (the so-called dendrochronology).

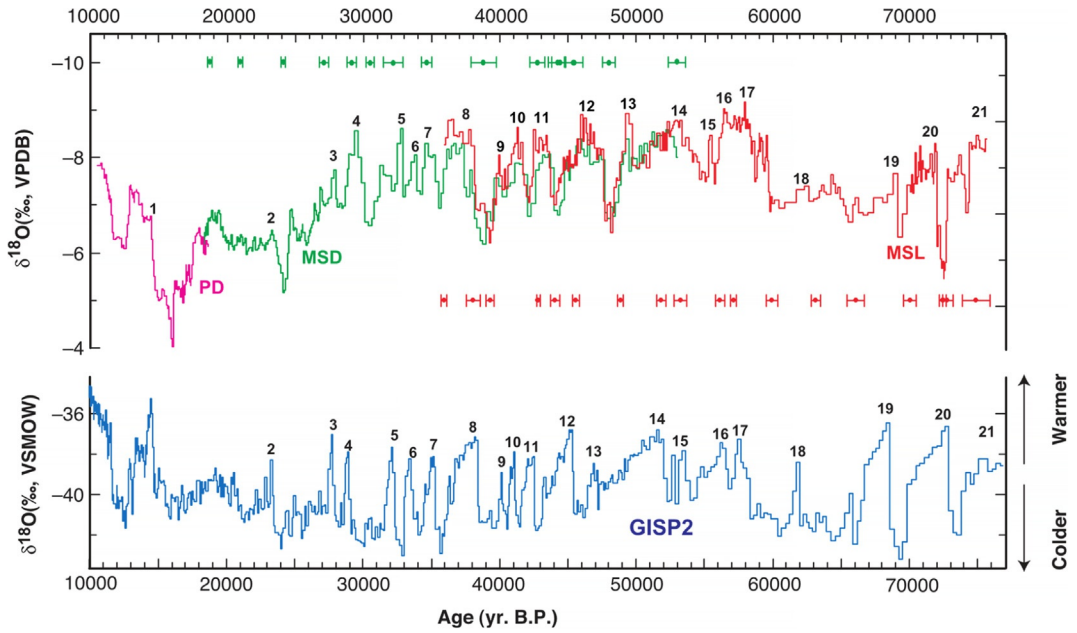

Fig. 6 D-O events recognized in speleothems from Hulu Cave (top) and in the isotopic composition of ice from GISP2 (bottom). The discrete markers with horizontal error bars represent the U/Th ages of the speleothems. Adapted from Wang YJ, Cheng H, Edwards RL, An ZS, Wu JY, Shen C-C, and Dorale JA (2001) A high-resolution absolute-dated late Pleistocene monsoon record from Hulu Cave, China. *Science* 294: 2345–2348. doi: https://doi.org/10.1126/science.1064618.

Impact of extraterrestrial objects

Impacts of large objects on the surface of the Earth are very distinct events and have the potential to be used as time horizons. Attempts have been made to find effects of the 1908 Tunguska Event. The term 'Tunguska Event' refers to a cosmic phenomenon observed on 30 June 1908 in Central Siberia over the Krasnoyarsk Territory, Irkutsk Region, when a large forest area was destroyed by the impact of a stellar object. The search for traces of iridium in a Greenland ice core from a large meteorite impact that may have caused the Tunguska event has failed. But some meteoritic events have been found in the ice core from EPICA Dome C around 450 kyr in the past.

Modelling of the sedimentation process

Given the knowledge of all material properties and boundary conditions, the plastic deformation and thermal properties of a glacier or ice sheet could be modelled. However, these boundary conditions and properties are generally poorly known. The bedrock topography, geothermal properties, subglacial sliding and oceanic conditions are not known in sufficient detail. Similarly, past surface conditions (temperature, precipitation) can only be indirectly estimated. The same holds for the parameters that determine flow properties, such as snow structure, crystal orientation, impurities, thermal properties, etc. Moreover, these numerical models have limited spatial and temporal resolution given their high computation cost. Therefore, only rough ice chronologies can be constructed using ice sheet models.

The problem of modelling the chronology of an ice core is often decomposed into 3 variables, surface accumulation rate, Lock-in-Depth and vertical thinning, which allow to determine the age scale relationships for the ice and for the air bubbles using the following 3 equations:

$$\chi(z) = \chi_0 + \int_{z_0}^{z} \frac{D(z')}{a(z')\tau(z')} dz', \tag{1}$$

$$\psi(z) = \chi\big(z - \Delta_{\mathrm{depth}}(z)\big), \tag{2}$$

$$\int_{z-\Delta_{\mathrm{depth}}(z)}^{z} \frac{D(z')}{\tau(z')} dz' = l(z) \times \frac{D}{\tau}\Big|_{firn}^{0}, \tag{3}$$

where z is the depth along the ice core record, $\chi(z)$ is the age of the ice at depth z, χ_0 is the age of the ice at the top (with depth $z = z_0$), a is the surface accumulation rate along the ice core, D is the relative density of the snow/ice material (dimensionless), τ is the

vertical thinning function (also dimensionless), Ψ is the age of the air, Δ_{depth} is the depth difference between air and ice of the same age, l is the lock-in-depth of air bubbles and $\frac{D}{T}|_{firn}^{0}$ is the average value of $\frac{D}{T}$ in the firn when the air particle was at the lock-in-depth.

The first equation integrates along the depth axis the number of annual layers per unit depth from the surface. The second equation means that the air age at depth z is equal to the ice age at depth $z - \Delta_{\text{depth}}$. This is the definition of Δ_{depth}. The third equation means that if one virtually un-thins a depth interval between an ice depth and the synchronous air depth, one gets the initial firn thickness in ice-equivalent units.

We will detail in the following how we estimate these three fundamental variables of the numerical age models (accumulation rate, Lock-in-Depth and thinning function).

Past accumulation rates estimates

Past accumulation rates are often assumed to be proportional to the derivative of the mean saturation vapor pressure at the inversion layer with respect to temperature. The inversion layer temperature is assumed to be linearly related to the surface temperature, which is itself estimated from the stable isotope ratio in the ice through a linear relationship. The isotopic content of ice can be corrected from the isotopic and temperature variations at the source of evaporation using the mean isotopic content of the ocean and using the deuterium excess content of the ice (Uemura et al., 2012).

An alternative approach for reconstructing paleoaccumulation rates is based on the concentration of trace substances in the ice. The net flux (atmosphere to ice) of any impurity is the product of the accumulation rate and the concentration in the ice. Past accumulation rates can thus be computed by measuring the concentrations and estimating the past fluxes. By this means, it has been possible to assess the accumulation rates for Central Greenland, using the cosmogenic radionuclides ^{10}Be and ^{36}Cl.

Snow densification and air trapping

The upper 50–120 m of an ice sheet is made of consolidated snow (firn) which is permeable to air (Fig. 2B). Air occluded at the firn–ice transition is therefore substantially younger than the ice. This age difference can be estimated with densification/diffusion models. The air at the firn-ice transition is on the order of one to a few decades. The age of the ice at the firn–ice transition spans a larger range of a few tens to several thousand years under present conditions, mainly depending on temperature and accumulation rates. Locations with high accumulation rates and relatively high annual temperatures show the smallest ages, while sites in central Antarctica with accumulation rates of few centimeters per year show the largest ages. The difference between the age of the ice and air has not remained constant over time. Under glacial conditions, this age difference was generally several times larger than at present.

The process of snow densification has been modelled using various approaches. One can cite the steady and empirical snow densification model of Herron and Langway (1980), which, despite of its simplicity, gives very accurate results and is still used nowadays in important applications. More complex snow densification models have been developed over the years, but the physics of porous material is a complex subject.

In firn models, the air trapping is usually modelled as a discrete Lock-in-Depth whose density is parametrized as a function of surface temperature or sometimes given by the Air Content measurements. In reality, the air trapping is a continuous process which happens over a depth range, and the difference in density of the snow layers induces per-layer locking and can even create air age reversals.

Aside from the firn models, it is also possible to determine the Lock-in-Depth of air bubbles using the gravitational fractionation in the firn. Indeed, below a convective zone of a few meters at most, molecular fractionation takes place in the so-called diffusive zone, where heavier isotopes are enriched proportionally to the height of this diffusive column (Landais et al., 2006). This way, Parrenin et al. (2013) were able to determine the relative phasing between Antarctic temperature and CO_2 variations during the last deglaciation using the EDC ice core.

Ice flow models

A variety of ice flow models can be used to deduce the vertical thinning function. We will describe a few examples ranging from the simplest to the most complex. Usually, these flow models deal with pure ice, that is, the firn is usually converted into pure ice by removing ~20–40 m to the surface elevation.

For an ice core drilled at a dome and assuming this dome has been stable in the past, a 1D vertical model can be used. Assuming the flow is completely steady, the vertical thinning function can be obtained by the following analytical formula:

$$\tau = (1 - \mu)\omega + \mu, \tag{4}$$

where ω is the horizontal flux shape function and $\mu = m/a$ is the ratio of basal melting over surface accumulation rate. The horizontal flux shape function can be determined using an analytical expression:

$$\omega(\zeta) = 1 - \frac{p+2}{p+1}(1 - \zeta) + \frac{1}{p+1}(1 - \zeta)^{p+2}, \tag{5}$$

where $\zeta = z/H$ is the normalized vertical coordinate (0 at bedrock and 1 at surface), and p a parameter modifying the non-linearity of ω (the smaller p, the more non-linear ω). It is also possible to add a basal sliding term to this equation. Johnsen and Dansgaard proposed another profile, where the vertical strain rate is constant in the upper part and decreases linearly in the bottom part.

The steady assumption for the surface accumulation rate and basal melting can be relaxed under the assumption they have common temporal variations:

$$\begin{aligned} a(x,t) &= \overline{a}(x)R(t), \\ m(x,t) &= \overline{m}(x)R(t), \end{aligned} \tag{6}$$

where $\overline{a}(x)$ and $\overline{m}(x)$ are the temporally averaged accumulation and melting rates at a certain point x. This is what we call the *pseudo-steady* assumption. In this case, the real age can be deduced from the steady age using the following change of variable:

$$d\chi_{\text{steady}} = R(t)d\chi. \tag{7}$$

When the ice core is situated on a flank of an ice sheet, such as at Vostok, it is possible to use a 2.5D model, assuming the flow line has been stable in the past.

When the problem is not pseudo-steady, for example when one wants to consider changes in surface/bedrock elevation or a change in the melting/accumulation ratio, the age equation needs to be solved using a numerical scheme which can be Lagrangian, Eulerian or semi-Lagrangian.

More complex 3D models with free surface can also be used, but usually with a coarse spatial grid, or with a higher resolution local model nested in a coarser global model.

Whatever dating model is used, there are poorly known parameters that induce a large uncertainty on the resulting modelled chronology. Given independent age controls on the chronology (given by methods described above), it is possible to constrain these poorly known parameters using optimization methods. For example, Parrenin et al. (2007) constrained the poorly known parameters of a 1D model applied to the EPICA Dome C and Dome Fuji ice cores. The same has been done with a more complex flow-line model applied to Vostok. However, this approach still has limitations because the assumptions of the model are often too simplistic and the resulting chronologies of different ice cores are sometimes incompatible.

Probabilistic models

All previously described dating methods have advantages and drawbacks. Since these different sources of information are often complementary, it is therefore beneficial to combine them. It is why an optimization method has been developed (IceChrono, Parrenin et al., 2015). It is based on the inversion of the 3 fundamental variables of the sedimentation model described above (surface accumulation rate, Lock-in-Depth and vertical thinning function). It is applied to several ice cores simultaneously, by using stratigraphic links that exist between these ice cores, dated horizons, intervals with known durations and observations of Δdepth (Fig. 7). This method has been used to obtain the reference chronology AICC2012 (Bazin et al., 2013), for 4 Antarctic ice cores (EDC, EDML, Vostok and TALDICE) and one Greenlandic ice core (NorthGRIP).

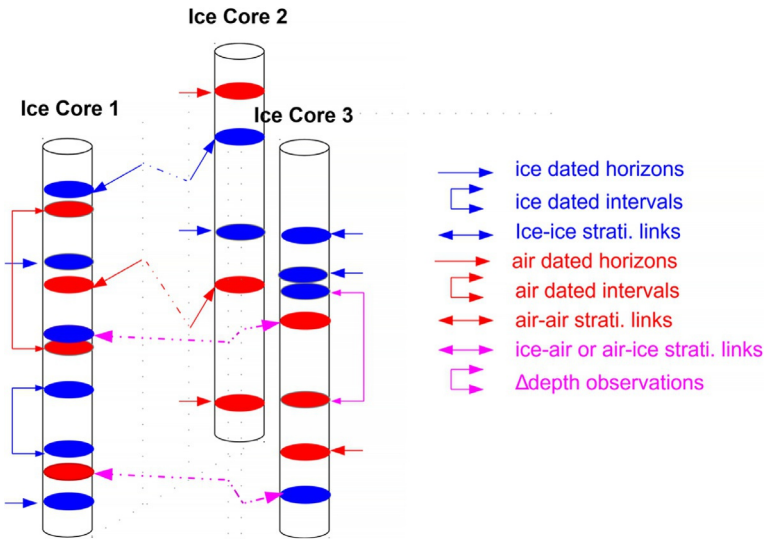

Fig. 7 Scheme illustrating the different types of chronological information used in probabilistic models to optimize the chronology of several ice cores at the same time. From Parrenin F, Bazin L, Capron E, Landais A, Lemieux-Dudon B, and Masson-Delmotte V (2015) IceChrono1: A probabilistic model to compute a common and optimal chronology for several ice cores. *Geoscientific Model Development* 8: 1473–1492. doi: https://doi.org/10.5194/gmd-8-1473-2015.

Conclusion

The dating of ice archives is a complex problem which, due to the absence of accurate radioactive methods, relies on several complementary techniques which can be combined using a probabilistic model.

For the Holocene, the layer counting chronologies GICC05 for Greenland and WD2014 for Antarctica are accurate within 1% and these chronologies have been confirmed with the comparison to dendrochronology using ^{10}Be or with dated volcanic eruptions. For the last glacial period, the accuracy of layer counted chronologies decreases but they are still valuable for constraining event durations. These chronologies are confirmed with independent U/Th dated speleothems, especially from Asia. Current principal dating methods for the last 60,000 years agree within a few centuries. These accurate chronologies can be transferred to East Antarctic ice cores using the methane records, although an evaluation of the ice-air age shift is necessary to deduce a chronology for the ice phase. Beyond the last glacial period, it is not possible to count layers and the ice cores chronologies relies on orbital tuning methods or to comparison with U/Th dated speleothems. These different methods largely agree within 2000 years.

References

Bazin L, Landais A, Lemieux-Dudon B, Toyé Mahamadou Kele H, Veres D, Parrenin F, Martinerie P, Ritz C, Capron E, Lipenkov V, Loutre M-F, Raynaud D, Vinther B, Svensson A, Rasmussen SO, Severi M, Blunier T, Leuenberger M, Fischer H, Masson-Delmotte V, Chappellaz J, and Wolff E (2013) An optimized multi-proxy, multi-site Antarctic ice and gas orbital chronology (AICC2012): 120–800 ka. *Climate of the Past* 9: 1715–1731. https://doi.org/10.5194/cp-9-1715-2013.

Bender ML (2002) Orbital tuning chronology for the Vostok climate record supported by trapped gas composition. *Earth and Planetary Science Letters* 204: 275–289. https://doi.org/10.1016/S0012-821X(02)00980-9.

Bender ML, Barnett B, Dreyfus G, Jouzel J, and Porcelli D (2008) The contemporary degassing rate of ^{40}Ar from the solid Earth. *Proceedings of the National Academy of Sciences* 105: 8232–8237. https://doi.org/10.1073/pnas.0711679105.

Corrick EC, Drysdale RN, Hellstrom JC, Capron E, Rasmussen SO, Zhang X, Fleitmann D, Couchoud I, and Wolff E (2020) Synchronous timing of abrupt climate changes during the last glacial period. *Science* 369: 963–969. https://doi.org/10.1126/science.aay5538.

EPICA Community Members, Barbante C, Barnola J-M, Becagli S, Beer J, Bigler M, Boutron C, Blunier T, Castellano E, Cattani O, Chappellaz J, Dahl-Jensen D, Debret M, Delmonte B, Dick D, Falourd S, Faria S, Federer U, Fischer H, Freitag J, Frenzel A, Fritzsche D, Fundel F, Gabrielli P, Gaspari V, Gersonde R, Graf W, Grigoriev D, Hamann I, Hansson M, Hoffmann G, Hutterli MA, Huybrechts P, Isaksson E, Johnsen S, Jouzel J, Kaczmarska M, Karlin T, Kaufmann P, Kipfstuhl S, Kohno M, Lambert F, Lambrecht A, Lambrecht A, Landais A, Lawer G, Leuenberger M, Littot G, Loulergue L, Lüthi D, Maggi V, Marino F, Masson-Delmotte V, Meyer H, Miller H, Mulvaney R, Narcisi B, Oerlemans J, Oerter H, Parrenin F, Petit J-R, Raisbeck G, Raynaud D, Röthlisberger R, Ruth U, Rybak O, Severi M, Schmitt J, Schwander J, Siegenthaler U, Siggaard-Andersen M-L, Spahni R, Steffensen JP, Stenni B, Stocker TF, Tison J-L, Traversi R, Udisti R, Valero-Delgado F, van den Broeke MR, van de Wal RSW, Wagenbach D, Wegner A, Weiler K, Wilhelms F, Winther J-G, and Wolff E (2006) One-to-one coupling of glacial climate variability in Greenland and Antarctica. *Nature* 444: 195–198. https://doi.org/10.1038/nature05301.

Extier T, Landais A, Bréant C, Prié F, Bazin L, Dreyfus G, Roche DM, and Leuenberger M (2018) On the use of $\delta^{18}O_{atm}$ for ice core dating. *Quaternary Science Reviews* 185: 244–257. https://doi.org/10.1016/j.quascirev.2018.02.008.

Herron MM and Langway CC (1980) Firn densification: An empirical model. *Journal of Glaciology* 25: 373–385. https://doi.org/10.3189/S0022143000015239.

Landais A, Barnola JM, Kawamura K, Caillon N, Delmotte M, Ommen TV, Dreyfus G, Jouzel J, Masson-Delmotte V, Minster B, Freitag J, Leuenberger M, Schwander J, Huber C, Etheridge D, and Morgan V (2006) Firn-air δ^{15}N in modern polar sites and glacial-interglacial ice: a model-data mismatch during glacial periods in Antarctica? *Quaternary Science Reviews* 25: 49–62. https://doi.org/10.1016/j.quascirev.2005.06.007.

Parrenin F, Dreyfus G, Durand G, Fujita S, Gagliardini O, Gillet F, Jouzel J, Kawamura K, Lhomme N, Masson-Delmotte V, Ritz C, Schwander J, Shoji H, Uemura R, Watanabe O, and Yoshida N (2007) 1-D-ice flow modelling at EPICA Dome C and Dome Fuji, East Antarctica. *Climate of the Past* 3: 243–259. https://doi.org/10.5194/cp-3-243-2007.

Parrenin F, Masson-Delmotte V, Köhler P, Raynaud D, Paillard D, Schwander J, Barbante C, Landais A, Wegner A, and Jouzel J (2013) Synchronous change of atmospheric CO_2 and Antarctic temperature during the last deglacial warming. *Science* 339: 1060–1063. https://doi.org/10.1126/science.1226368.

Parrenin F, Bazin L, Capron E, Landais A, Lemieux-Dudon B, and Masson-Delmotte V (2015) IceChrono1: A probabilistic model to compute a common and optimal chronology for several ice cores. *Geoscientific Model Development* 8: 1473–1492. https://doi.org/10.5194/gmd-8-1473-2015.

Raisbeck GM, Yiou F, Jouzel J, and Stocker TF (2007) Direct north-south synchronization of abrupt climate change record in ice cores using Beryllium 10. *Climate of the Past* 3: 541–547. https://doi.org/10.5194/cp-3-541-2007.

Raynaud D, Lipenkov V, Lemieux-Dudon B, Duval P, Loutre M-F, and Lhomme N (2007) The local insolation signature of air content in Antarctic ice. A new step toward an absolute dating of ice records. *Earth and Planetary Science Letters* 261: 337–349. https://doi.org/10.1016/j.epsl.2007.06.025.

Severinghaus JP, Sowers T, Brook EJ, Alley RB, and Bender ML (1998) Timing of abrupt climate change at the end of the Younger Dryas interval from thermally fractionated gases in polar ice. *Nature* 391: 141–146. https://doi.org/10.1038/34346.

Sigl M, Winstrup M, McConnell JR, Welten KC, Plunkett G, Ludlow F, Büntgen U, Caffee M, Chellman N, Dahl-Jensen D, Fischer H, Kipfstuhl S, Kostick C, Maselli OJ, Mekhaldi F, Mulvaney R, Muscheler R, Pasteris DR, Pilcher JR, Salzer M, Schüpbach S, Steffensen JP, Vinther BM, and Woodruff TE (2015) Timing and climate forcing of volcanic eruptions for the past 2,500 years. *Nature* 523: 543–549. https://doi.org/10.1038/nature14565.

Sigl M, Fudge TJ, Winstrup M, Cole-Dai J, Ferris D, McConnell JR, Taylor KC, Welten KC, Woodruff TE, Adolphi F, Bisiaux M, Brook EJ, Buizert C, Caffee MW, Dunbar NW, Edwards R, Geng L, Iverson N, Koffman B, Layman L, Maselli OJ, McGwire K, Muscheler R, Nishiizumi K, Pasteris DR, Rhodes RH, and Sowers TA (2016) The WAIS Divide deep ice core WD2014 chronology – Part 2: Annual-layer counting (0–31 ka BP). *Climate of the Past* 12: 769–786. https://doi.org/10.5194/cp-12-769-2016.

Svensson A, Andersen KK, Bigler M, Clausen HB, Dahl-Jensen D, Davies SM, Johnsen SJ, Muscheler R, Parrenin F, Rasmussen SO, Röthlisberger R, Seierstad I, Steffensen JP, and Vinther BM (2008) A 60 000 year Greenland stratigraphic ice core chronology. *Climate of the Past* 4: 47–57. https://doi.org/10.5194/cp-4-47-2008.

Svensson A, Dahl-Jensen D, Steffensen JP, Blunier T, Rasmussen SO, Vinther BM, Vallelonga P, Capron E, Gkinis V, Cook E, Kjær HA, Muscheler R, Kipfstuhl S, Wilhelms F, Stocker TF, Fischer H, Adolphi F, Erhardt T, Sigl M, Landais A, Parrenin F, Buizert C, McConnell JR, Severi M, Mulvaney R, and Bigler M (2020) Bipolar volcanic synchronization of abrupt climate change in Greenland and Antarctic ice cores during the last glacial period. *Climate of the Past* 16: 1565–1580. https://doi.org/10.5194/cp-16-1565-2020.

Uemura R, Masson-Delmotte V, Jouzel J, Landais A, Motoyama H, and Stenni B (2012) Ranges of moisture-source temperature estimated from Antarctic ice cores stable isotope records over glacial–interglacial cycles. *Climate of the Past* 8: 1109–1125. https://doi.org/10.5194/cp-8-1109-2012.

Wang YJ, Cheng H, Edwards RL, An ZS, Wu JY, Shen C-C, and Dorale JA (2001) A high-resolution absolute-dated late Pleistocene monsoon record from Hulu Cave, China. *Science* 294: 2345–2348. https://doi.org/10.1126/science.1064618.